Energy Materials

Supplemental Materials

In-situ polymerized and crosslinked electrolytes with interchangeable Li/Na transport for battery applications

Harmandeep Singh[1], Josh T. Damron[2], M Shahriar[3,4], Mary Danielson[2], Rob Beard[2], Rachel Eberhard[2], Georgios Polizos[3], Ivan Popov[5], Md Anisur Rahman[2,*], Alexei P. Sokolov[2,6], Catalin Gainaru[2,*]

[1]Bredesen Center for Interdisciplinary Research and Graduate Education, University of Tennessee, Knoxville, TN 37996, USA.

[2]Chemical Sciences Division, Oak Ridge National Laboratory, Oak Ridge, TN 37831, USA.

[3]Electrification and Energy Infrastructures Division, Oak Ridge National Laboratory, Oak Ridge, TN 37831, USA.

[4]Department of Mechanical Engineering, Iowa State University, Iowa, IA 50010, USA.

[5]University of Tennessee - Oak Ridge Innovation Institute, University of Tennessee, Knoxville, TN 37996, USA.

[6]Department of Chemistry, University of Tennessee, Knoxville, TN 37996, USA.

[*]**Correspondence to:** Dr. Md. Anisur Rahman and Dr. Catalin Gainaru, Chemical Sciences Division, Oak Ridge National Laboratory, Oak Ridge, TN 37831, USA. E-mail rahmana1@ornl.gov; gainarucp@ornl.gov

A. NMR results

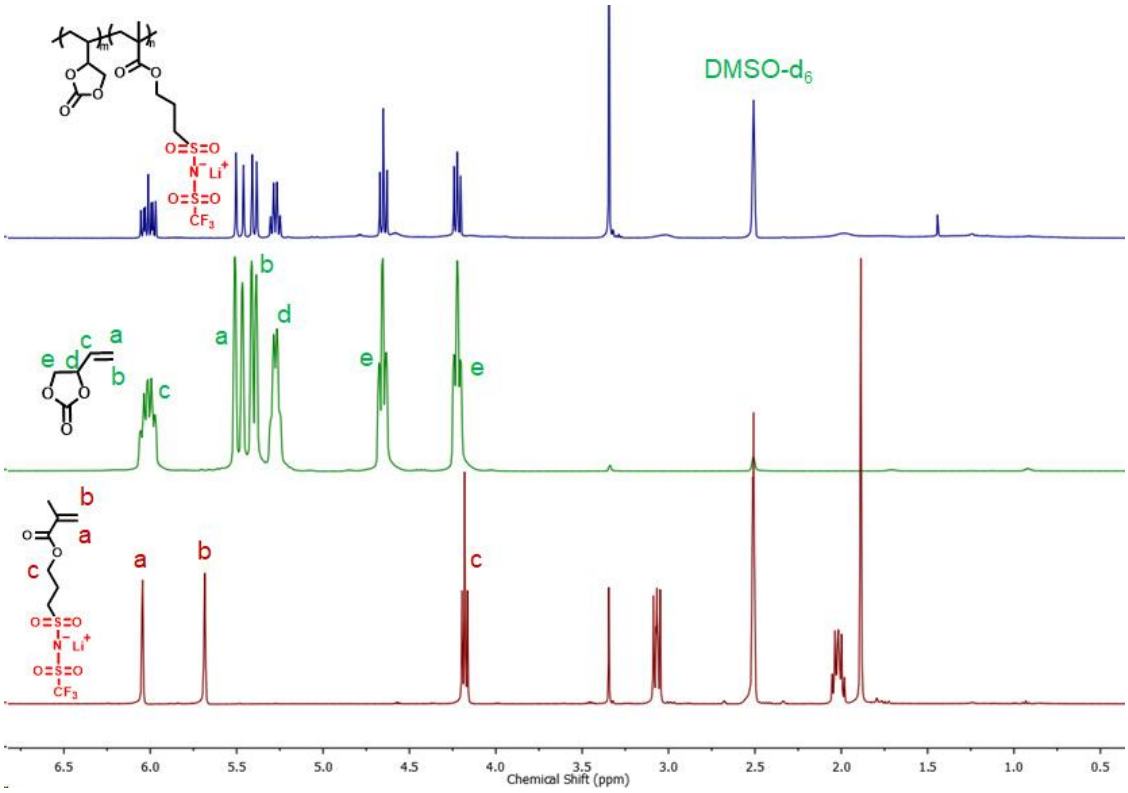

Fig. S1 1H NMR spectra of monomers, LiMTFSI and VEC, as well as copolymer in DMSO-d6. The NMR spectra show near completion of the polymerization of LiMTFSI (peak a and b in the spectra of MTFSI disappears in copolymers). The amount of polymerized VEC is estimated to be ~40% by measuring the integration.

B. Temperature-dependent DC conductivity of Li electrolyte

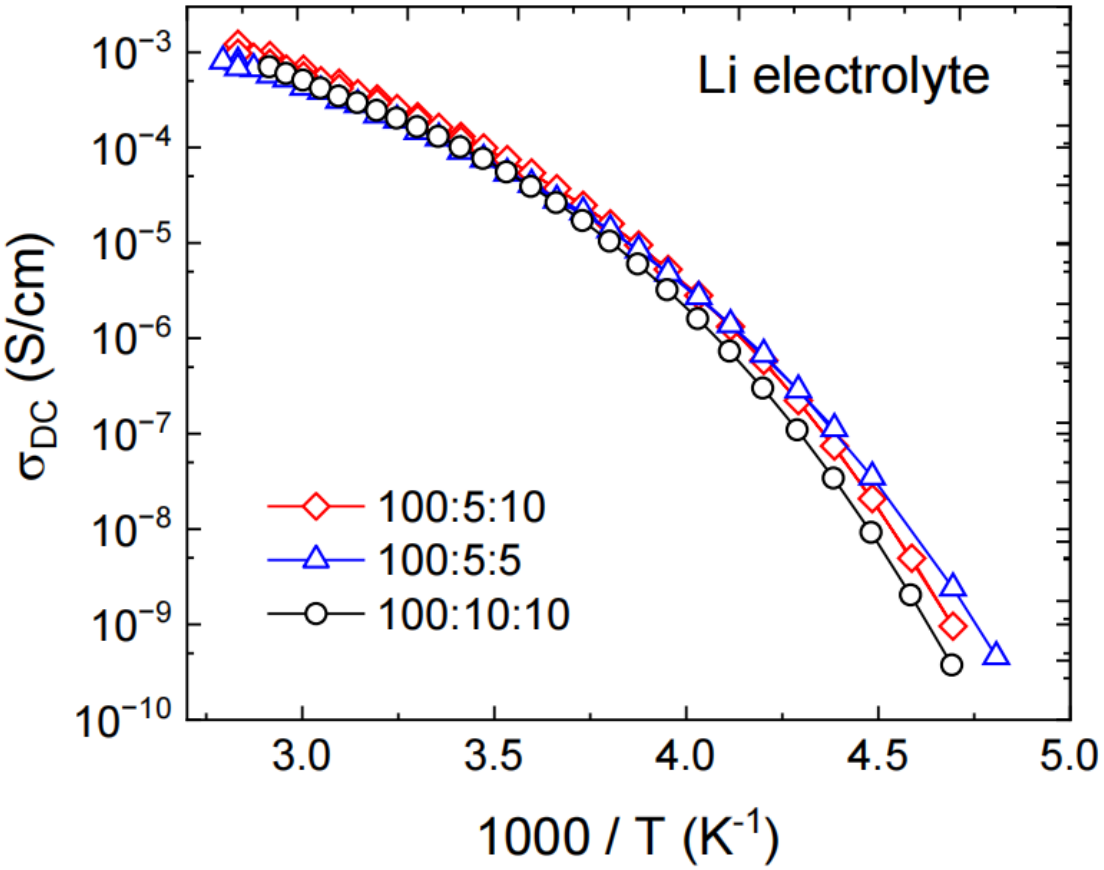

Fig. S2 Temperature dependence of the DC conductivity probed for the Li electrolyte with different [VEC]:[MTFSI$^-$]:[LiTFSI] compositions

C. Conductivity spectra of Li and Na electrolytes

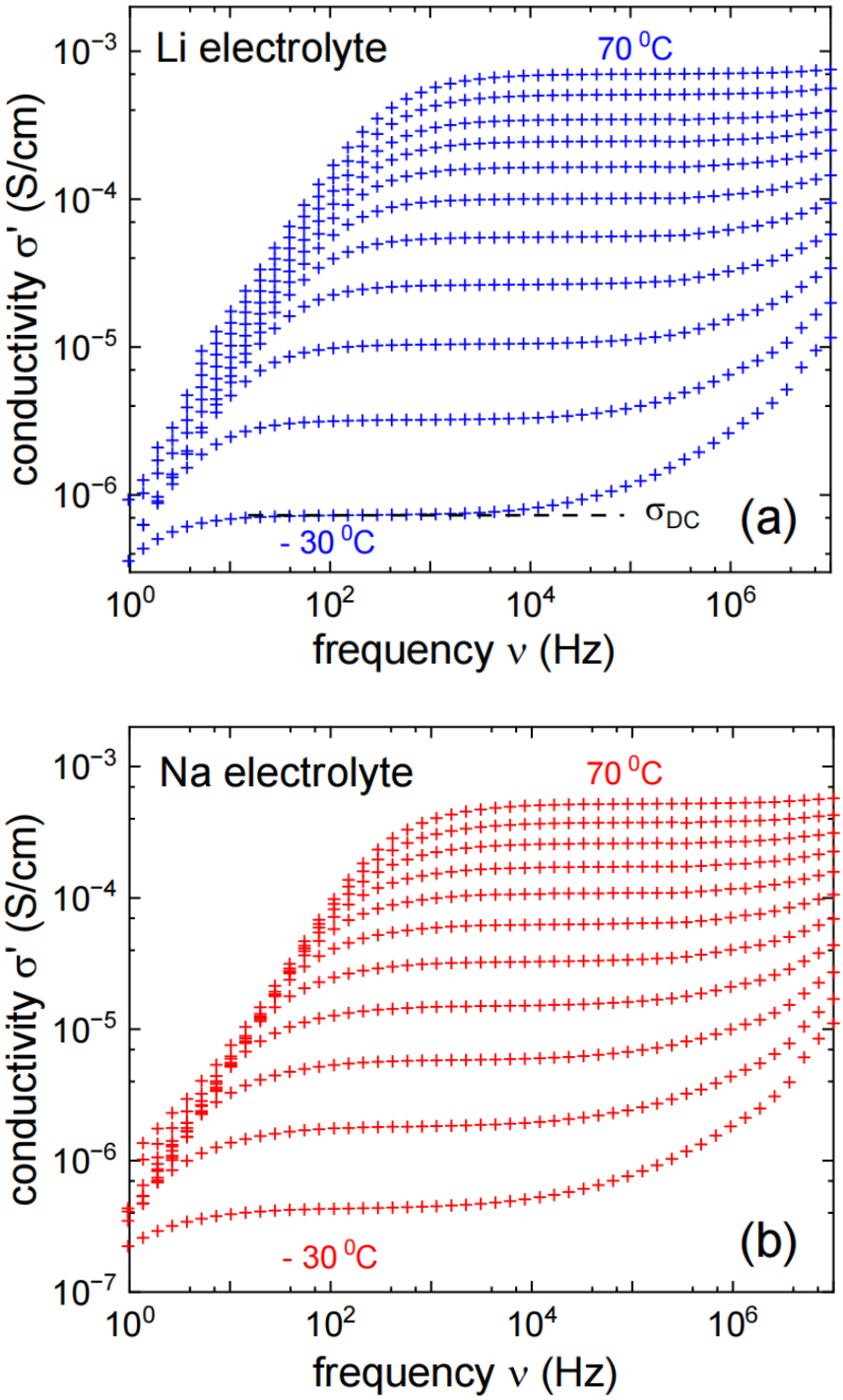

Fig. S3 Frequency-dependent conductivity σ' probed for (a) Li electrolyte (composition [VEC]:[MTFSI$^-$]:[LiTFSI]=100:10:10) and (b) Na electrolyte (composition [VEC]:[MTFSI$^-$]:[NaTFSI]=100:10:10) in temperature steps of 10 ºC.

D. Estimation of $t+,I$ for the Li electrolyte

To estimate $t+,I$ we used the data shown in Fig. 5a of the main manuscript. In Fig. S3 we are reproducing the same plots indicating the $R,0$ [corresponding to low Re(z) regime] and R,SS [corresponding to high Re(z) regime] parameters.

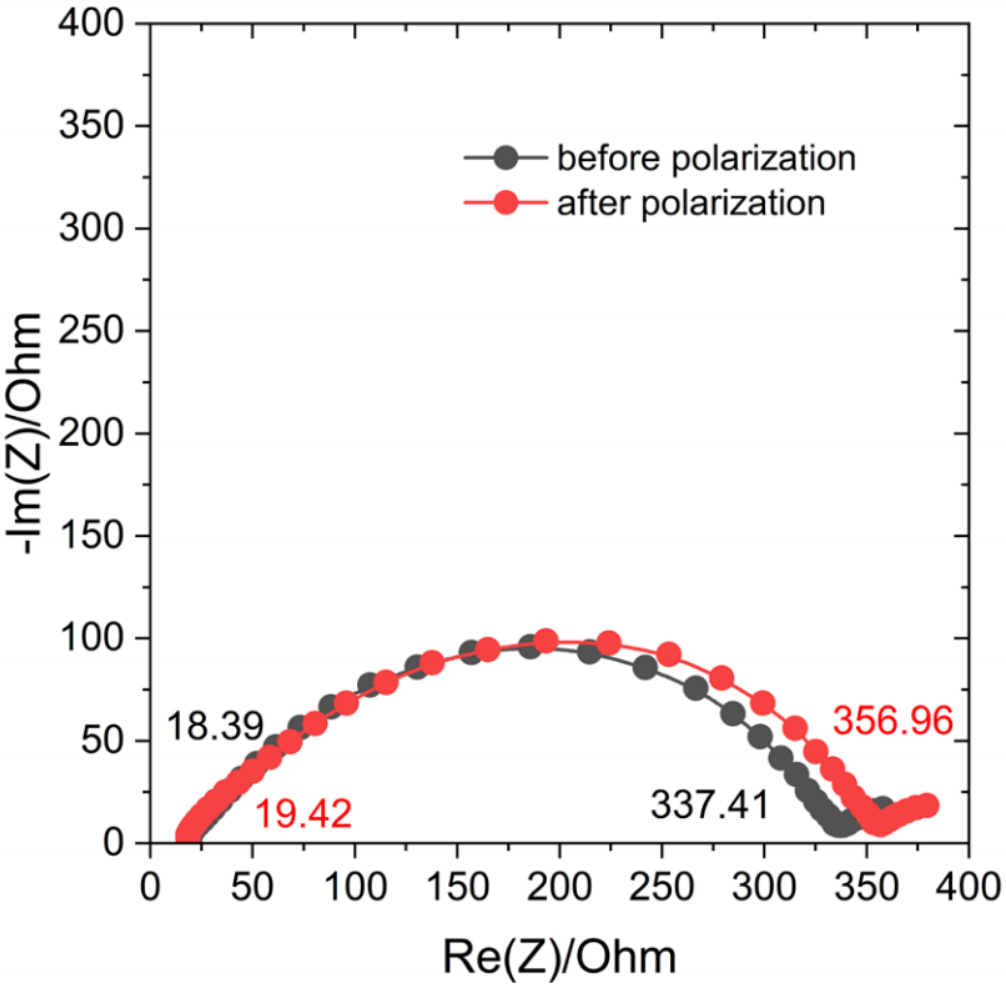

Fig. S4 Nyquist plots obtained before (black symbols) and after (red symbols) polarization. The *Iss* and *I0* parameters are indicated in Fig. S4 and short, and respectively long times. ΔVV=10 V

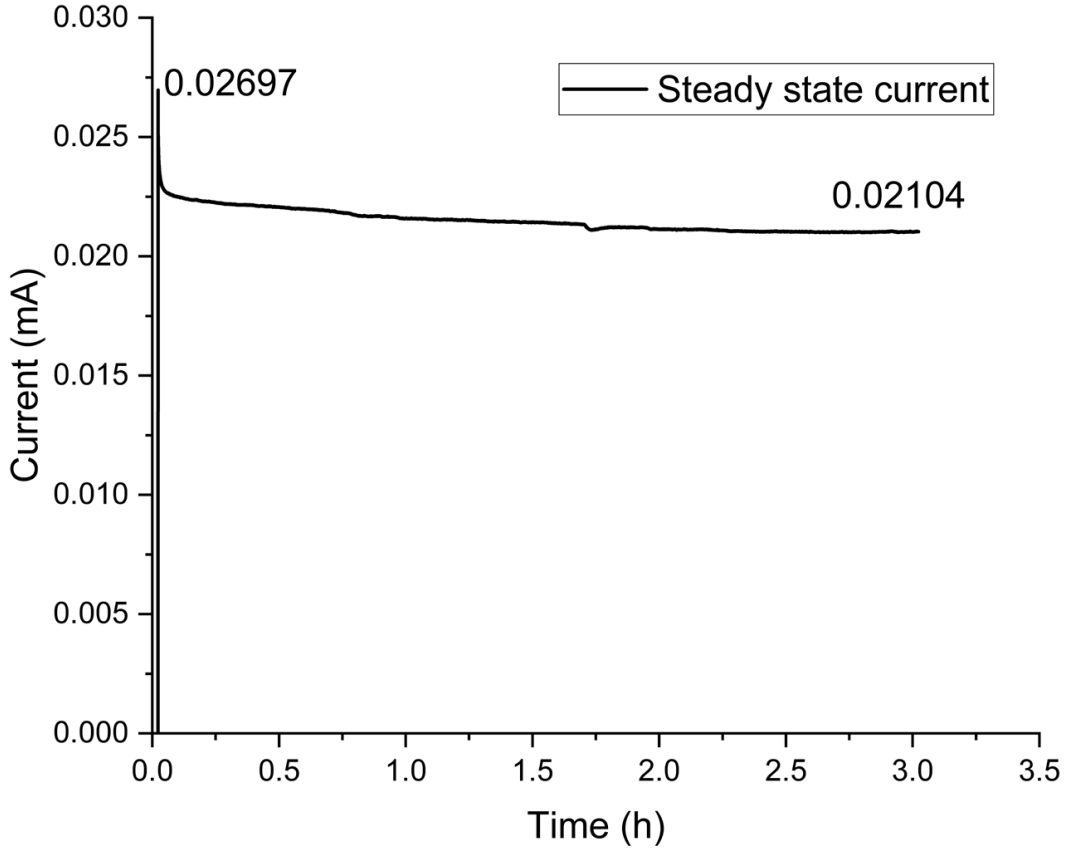

Fig. S5 Time evolution of the current during the Bruce-Vincent test.

$$t_+ = \frac{I_{ss}(\Delta V - I_0 R_{,0})}{I_0(\Delta V - I_{ss} R_{,ss})} = \frac{0.02104(10 - 0.02697 * 317.99)}{0.02697(10 - 0.02104 * 338.57)} \sim 0.4$$

E. Further cell testing results

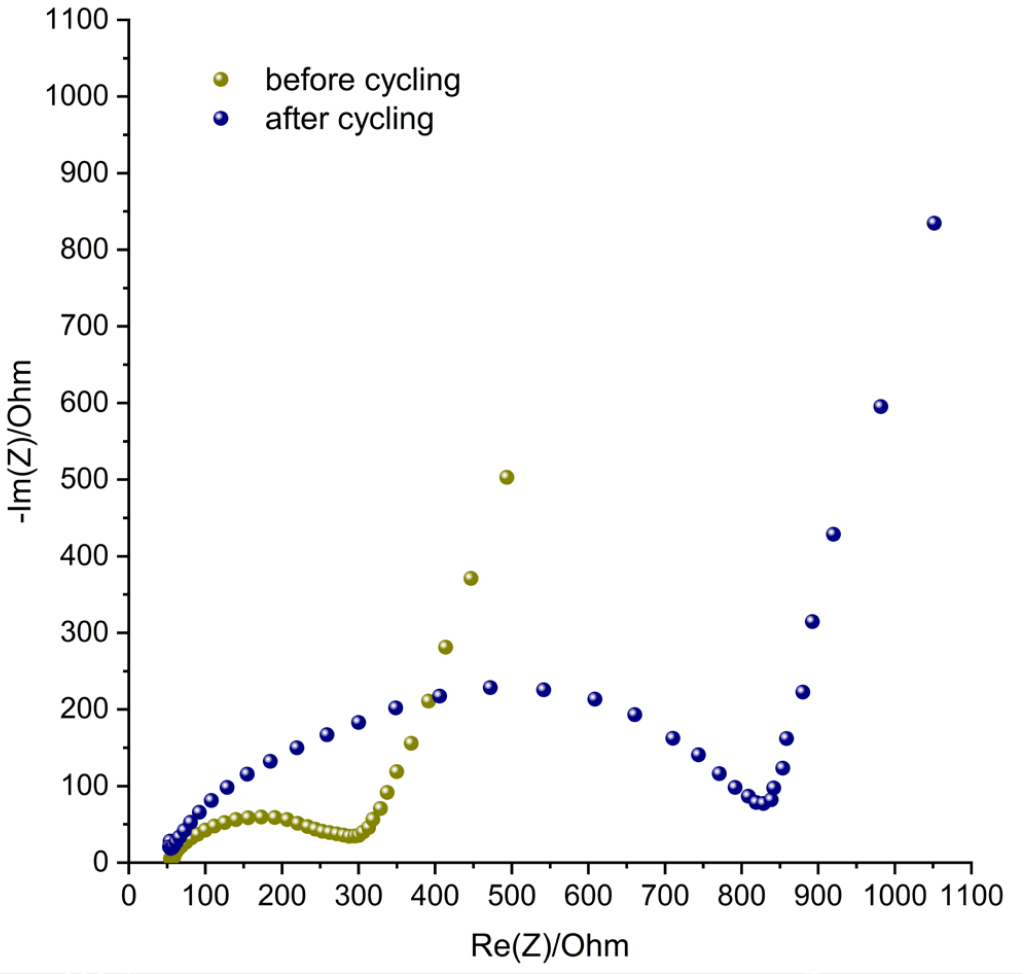

Fig. S6 Nyquist plot before and after cycling for the LFP cell with results shown in Figure 6a of the manuscript.

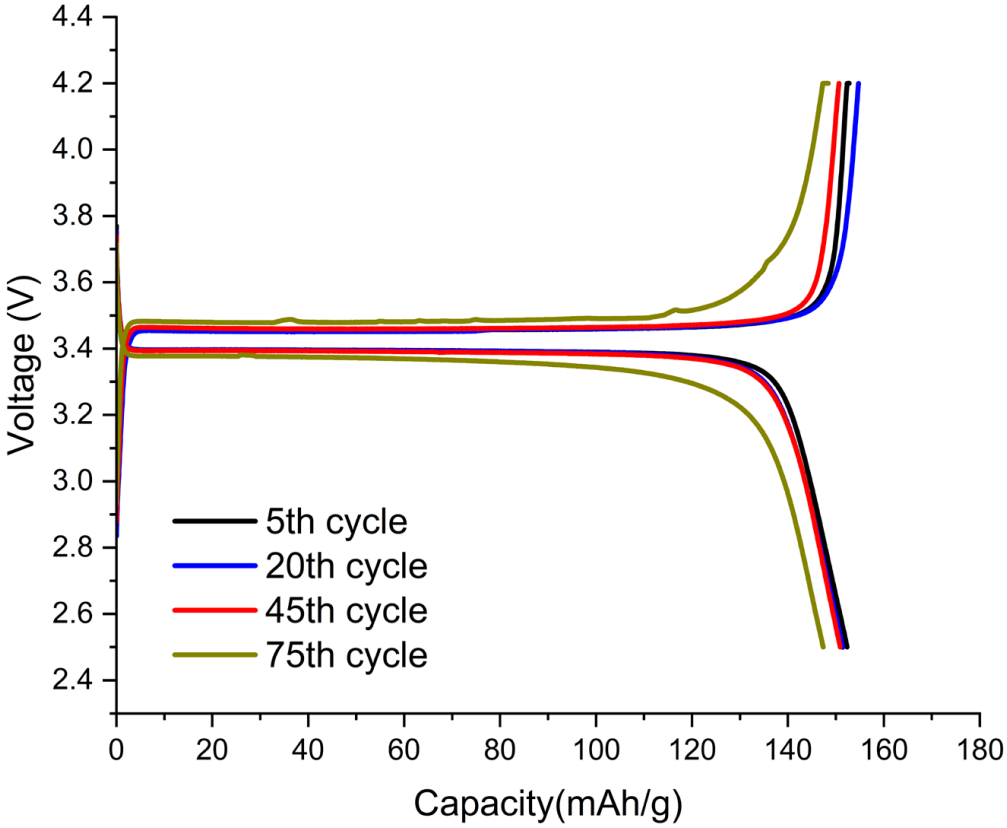

Fig. S7 Voltage versus specific capacity profile for the LFP cell in Figure 6a.

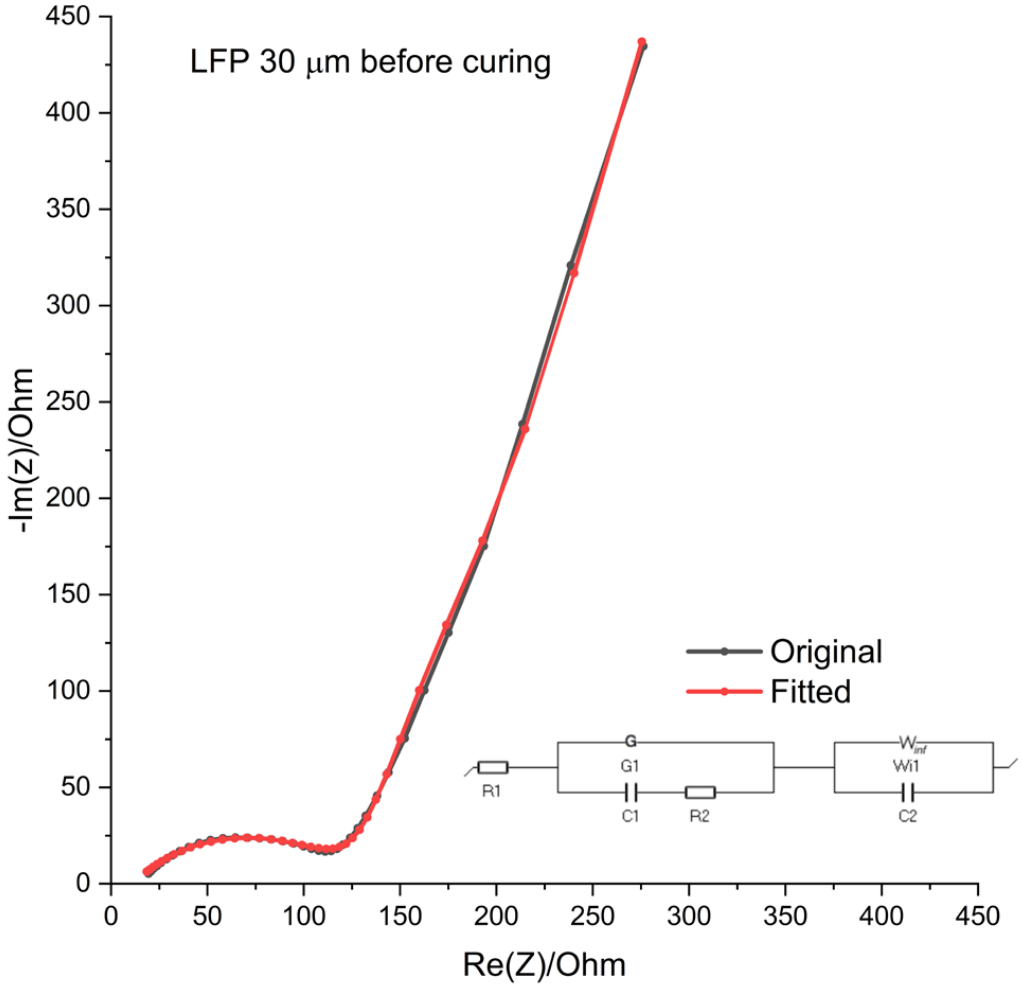

Fig. S8 Nyquist plot and fitting curve for the LFP cell in Figure 6a before curing. The equivalent circuit that was used for the fitting is also shown on the plot.

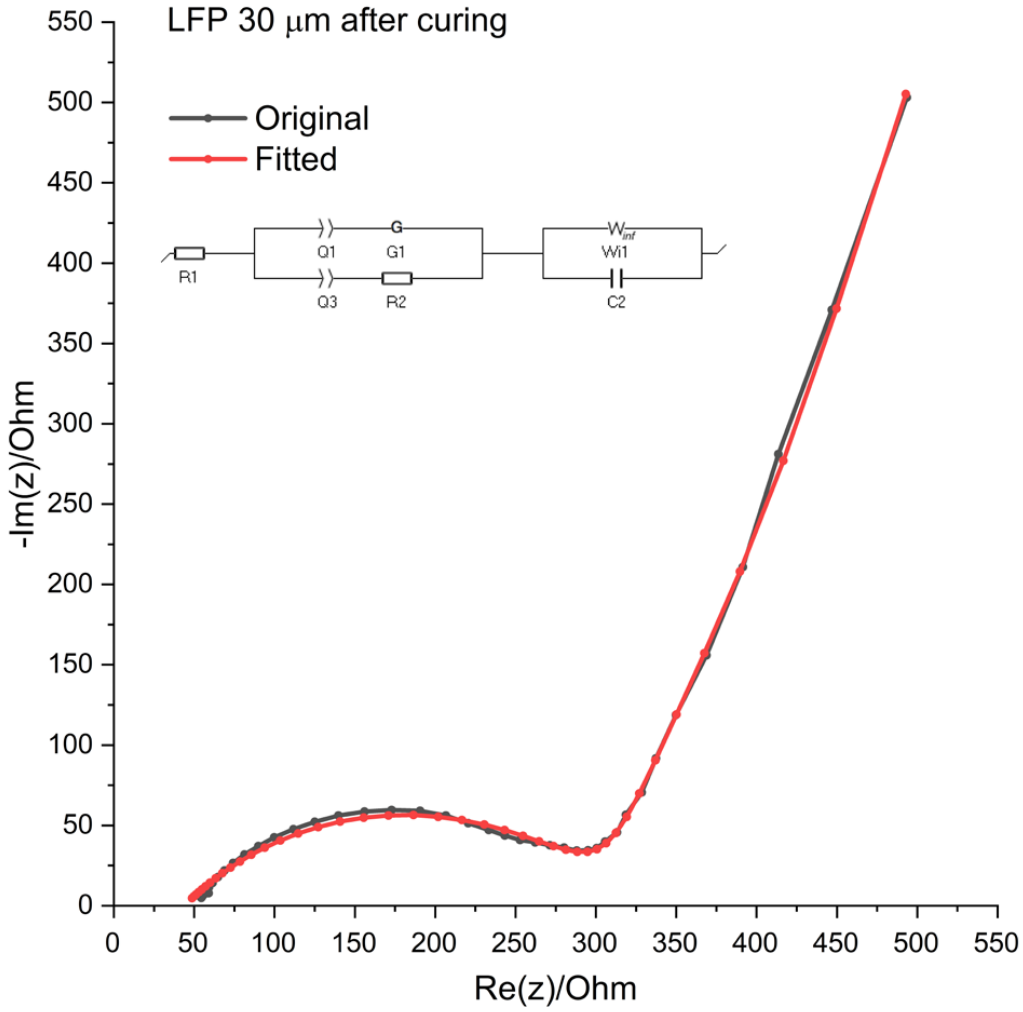

Fig. S9 Nyquist plot and fitting curve for the LFP cell in Figure 6a after curing and before cycling. The equivalent circuit that was used for the fitting is also shown on the plot.

To obtain the best fitting results in Figs S9 and S10 a Gerischer impedance (G) was used in the equivalent circuit indicating the presence of heterogeneous reactions at the interfaces between the electrodes and the electrolyte.

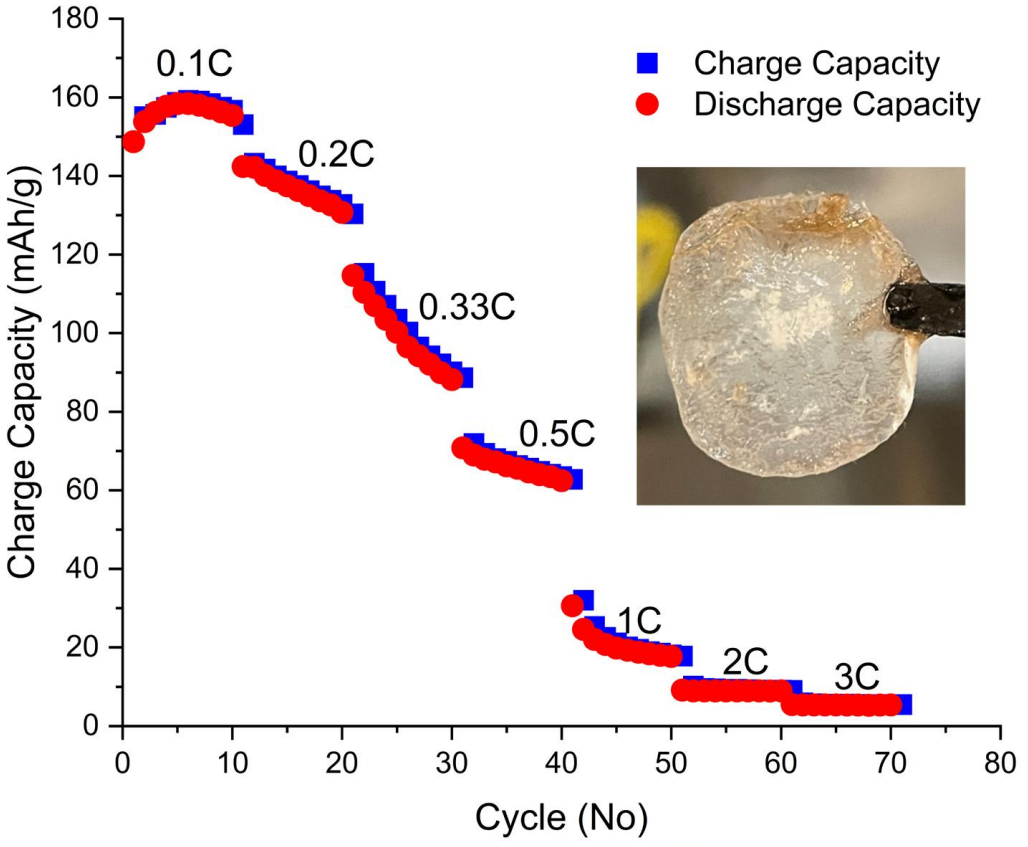

Fig. S10 C-rate capability of the NMC 622 non-crosslinked cell at 30 ^{o}C. The active material loading was 2.26 mg/cm^{2}. The inset image shows the electrolyte/Celgard 2325 separator after cycling. The separator is free-standing with no obvious discoloration due to degradation in the center of the disc that was in contact with the Li metal anode.